



Student Name: Douglas Beaton

FINAL PROJECT REPORT

COURSE NO.: MUMT 618

COURSE NAME: Computational Modeling of Musical Acoustic Systems

LAB/ASSIGNMENT NO.: Final Project

NAME OF INSTRUCTOR: Dr. Scavone

Date of Submission: Dec 5 '18 Due Date: Dec 11 '18

For use by marker

Marked by:

Mark:

3D Finite Element Modal Analysis of a Marimba Bar

Background

This project is based on work described in “Comparison Between Modal Analysis and Finite Element Modelling of a Marimba Bar” by Bork et al. [1] (referred to as ‘the paper’ throughout this report). The paper outlines the results of an experimental modal analysis of a marimba bar and compares them with finite element predictions. Measured and predicted modal frequencies are reported for the first 25 modes of the bar, with some appearing in only the experimental or simulation results, but not both. Mode shapes are plotted and compared for those modes appearing in both sets of results. The resulting modal frequencies agree to within 4%, up to a frequency of 4 kHz.

Objectives

The objective of this work is to reproduce the marimba bar model described by Bork et al. [1] in the open-source finite element software *Calculix*. A modal analysis is performed on the finite element model to estimate the bar's natural frequencies and mode shapes. These results are then compared with the published values in the paper [1]. The model's mesh density is then varied to assess convergence of the results.

Methodology

Software

To facilitate rapid variations in mesh densities and geometry, a partial interface was implemented between *Calculix*, and the author's own finite element pre- and post-processor, *Pylaster*. This interface allows model geometry to be defined parametrically in *Pylaster*, which uses the Python programming language. The interface then creates a *Calculix* input (.inp) file, sends a command to run the model, reads the *Calculix* output (.dat) file, and either reports results in Python or exports files for visualization in the open-source package *Paraview*. Using this framework, mesh densities can easily be varied to perform convergence tests. This setup also enables iterative model tuning, with model inputs adjusted based on previous outputs, and algorithms implemented to tune the bar for a desired response.

Geometry

Bork et al. [1] provide most, but not all, of the geometry required to reproduce their finite element model. A precise definition of the bar's "undercut" is not provided. The paper noted that the undercut thickness varied between 10-20% along the longitudinal axis and that these variations were not symmetric. The thickness of the undercut is reported to have been modelled as "equal to the mean value of the measured thicknesses" [1]. No further elaboration is provided.

All of the model information provided by the paper was incorporated in the model produced for this work. In addition, the following assumptions or approximations were made:

- A) Variable element spacing in the longitudinal direction was approximated by scaling dimensions and counting elements in Figure 1.
- B) The central portion of the bar, with the tightest element spacing, was assumed to be a constant thickness, equal to the minimum thickness reported in Table 1.

- C) Local axes for the orthotropic material definition were assumed to correspond to the bar's local axes as follows:
- Material longitudinal axis = bar longitudinal axis.
 - Material radial axis = bar vertical axis.
 - Material tangential axis = bar transverse axis.

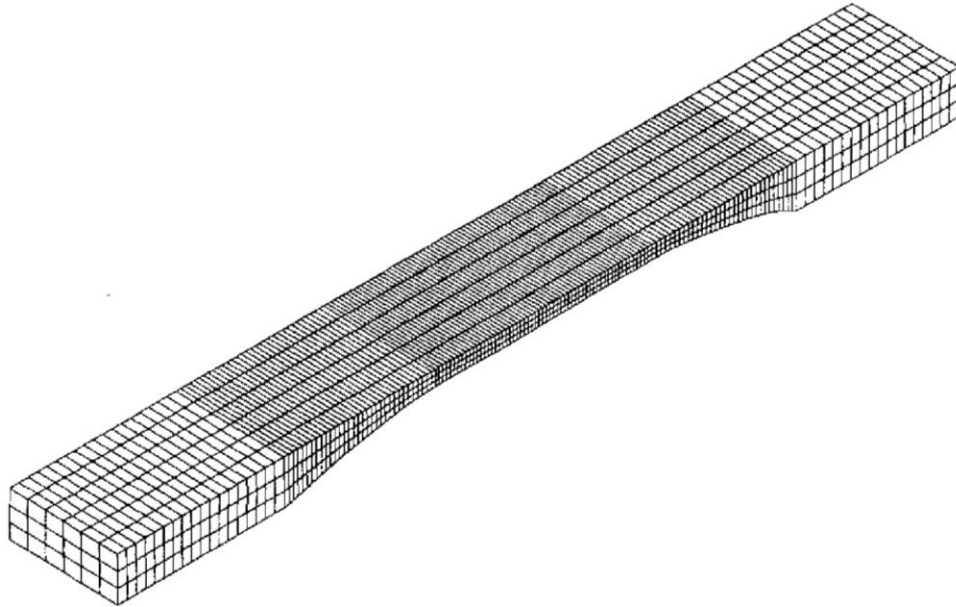


Figure 1: Finite element mesh of the original bar model (Figure 9 in Bork et al. [1])

Model Tuning

After making the assumptions and approximations outlined above, it remained to define the geometry of the transition zones between the ends of the bar (which have the maximum thickness) and the centre portion (with minimum thickness). Two transition profiles were investigated. In each case a single control point was defined midway through the transition (see Figure 2). The bar's thickness at this control point was used along with the known thicknesses at each end to define the transition profile. A parabolic profile was investigated first, followed by a cubic profile. The additional term in the cubic profile was defined by setting the slope of the undercut to zero where the transition meets the centre portion of the bar.

For each of the profiles considered, the bar's thickness at the control point was determined by tuning the overall mass of the model to match that reported in Table 1. Once the profile was set by tuning the bar's overall mass, modal analyses were performed to determine the bar's natural frequencies and mode shapes.

Additional investigations were performed using multiple transition zone control points, with piecewise cubic interpolation, to attempt to tune modal frequencies along with the bar mass. Tuning the bar in this manner is beyond the scope of this project, thus the results of these attempts are omitted here.

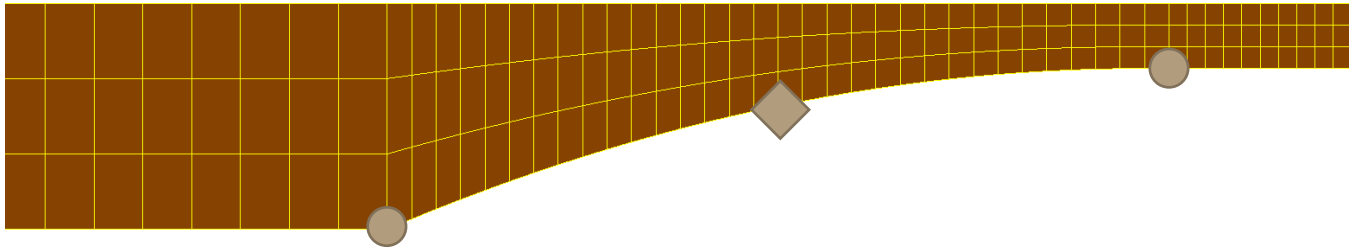


Figure 2: Detailed view of the transition between portions of the bar with uniform thickness. Shown in grey are the end points (circles) and control point (diamond).

Table 1: Bar dimensions and material properties from Bork et al. [1]

Length	46.0 cm
Width	6.0 cm
Maximum thickness	2.35 cm
Minimum thickness	0.68 cm
Total mass	457.8 g
Young's modulus (longitudinal)	23 GPa
Young's modulus (radial)	2.3 GPa
Young's modulus (tangential)	1.15 GPa
Density	1080 kg/m ³
Poisson's ratio (longitudinal-radial)	0.3
Poisson's ratio (radial-tangential)	0.6
Poisson's ratio (longitudinal-tangential)	0.45
Shear modulus (longitudinal-radial)	3.0 GPa
Shear modulus (radial-tangential)	1.0 GPa
Shear modulus (longitudinal-tangential)	3.0 GPa
Number of elements along length	160
Number of elements along width	6
Number of elements through thickness	3
Total number of elements	2880

Convergence Tests

After tuning the transition zones using the same finite element mesh described in the paper, convergence tests were performed by increasing or decreasing the number of elements along one or more of the global axes. A first set of tests varied only the number of elements in the longitudinal direction. A second set of tests varied the number of elements in the transverse and vertical directions simultaneously.

Results

Transition Tuning

Differences in modal frequencies using the cubic transition profile vs. the parabolic transition profile were found to be negligible. This result is not surprising, as a plot of the two tuned profiles must be magnified to a great extent before any difference in the profiles can be seen. To avoid repetition, only results from the mode with cubic transition zones are reported below.

Mode Shapes and Frequencies

Figure 3 compares modal frequencies calculated by the finite element analysis in this work, as well as that in the paper, to the experimental modal frequency measurements from the paper. Figure 4 plots the relative error between the finite element analyses and the measured values from the paper. Numerical values for the data in these two figures are provided in Table 2.

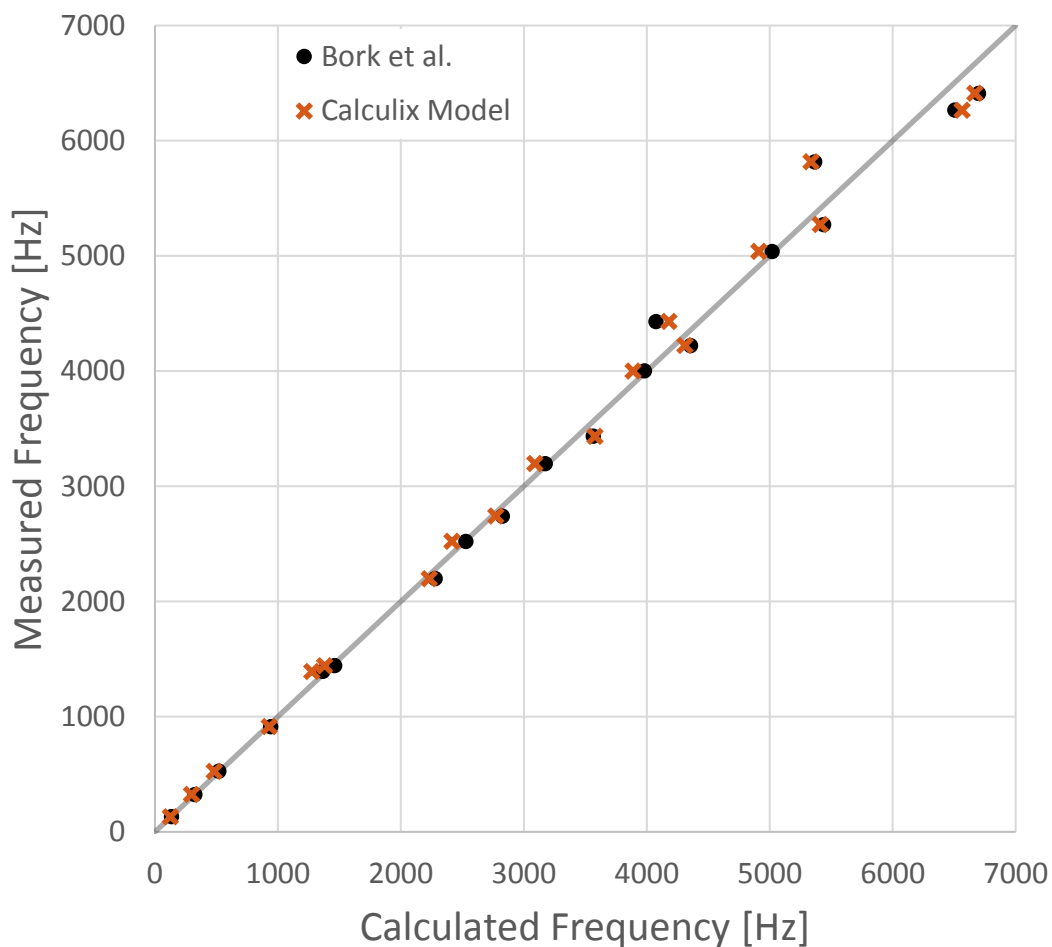


Figure 3: Modal frequency results. Modelling results from this work and the paper are each compared to the experimental modal analysis results from the paper (see also Figure 11 from Bork et al. [1]).

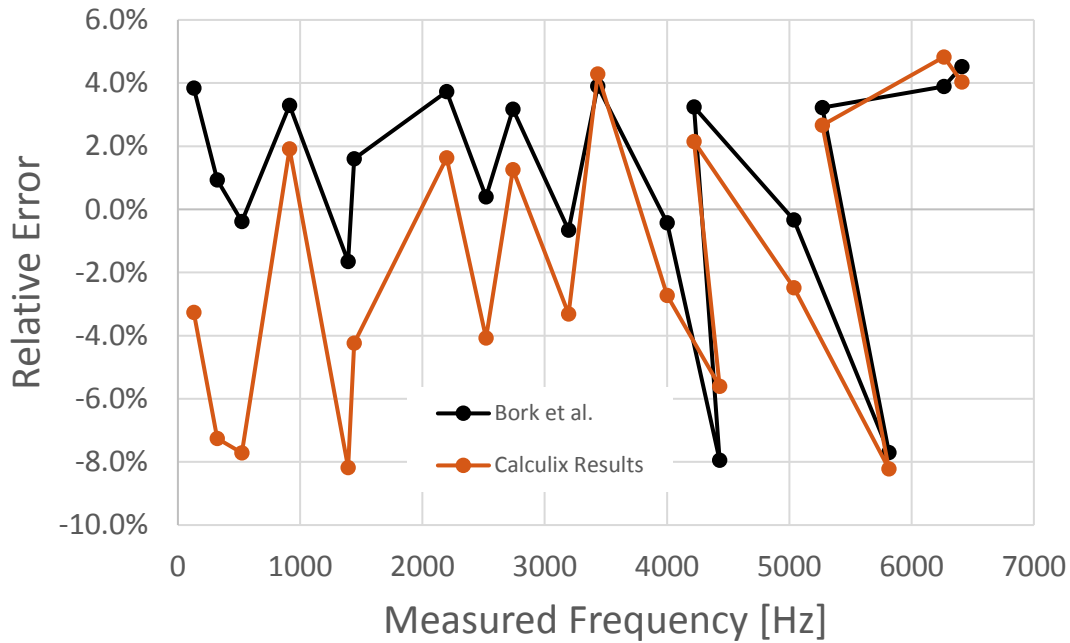


Figure 4: Relative error between finite element modal frequencies and measured values reported by Bork et al. [1]

Table 2: Comparison of measured and calculated modal frequencies. Only those modes with both measured and modelled results in the paper are shown (see also, Table II in Bork et al. [1])

Mode #	Modal Frequencies [Hz]				
	Bork et al.			Calculix Results	
	Measured	FE Model	Error	FE Model	Error
1	130	135	3.8%	126	-3.3%
2	323	326	0.9%	300	-7.3%
3	524	522	-0.4%	484	-7.7%
4	912	942	3.3%	930	1.9%
5	1391	1368	-1.7%	1277	-8.2%
6	1441	1464	1.6%	1380	-4.2%
7	2197	2279	3.7%	2233	1.6%
8	2520	2530	0.4%	2417	-4.1%
9	2740	2827	3.2%	2774	1.3%
10	3196	3175	-0.7%	3090	-3.3%
11	3433	3567	3.9%	3580	4.3%
12	4000	3983	-0.4%	3891	-2.7%
13	4429	4077	-7.9%	4181	-5.6%
15	4221	4358	3.2%	4312	2.1%
16	5037	5020	-0.3%	4912	-2.5%
17	5815	5367	-7.7%	5337	-8.2%
18	5271	5441	3.2%	5411	2.7%
22	6264	6508	3.9%	6566	4.8%
23	6410	6700	4.5%	6669	4.0%

Figure 5 through Figure 7 show mode shapes from Calculix for the three tuned vertical modes of the marimba bar, while Figure 8 and Figure 9 show higher-order torsional mode shapes. The plots employ a hot-cold colour map of the overall magnitude of displacement at each point. Blue areas represent minimum displacement, red areas represent maximum displacement, and white areas represent intermediate displacement.

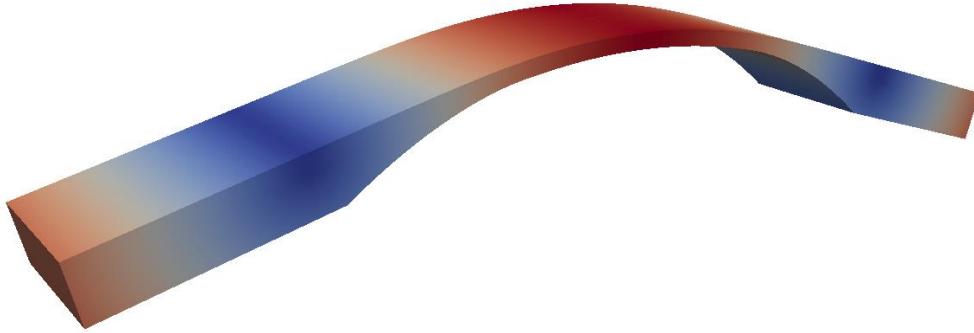


Figure 5: Mode shape #1 from Calculix. The hot-cold colour map indicates overall displacement from blue (minimum) to red (maximum).

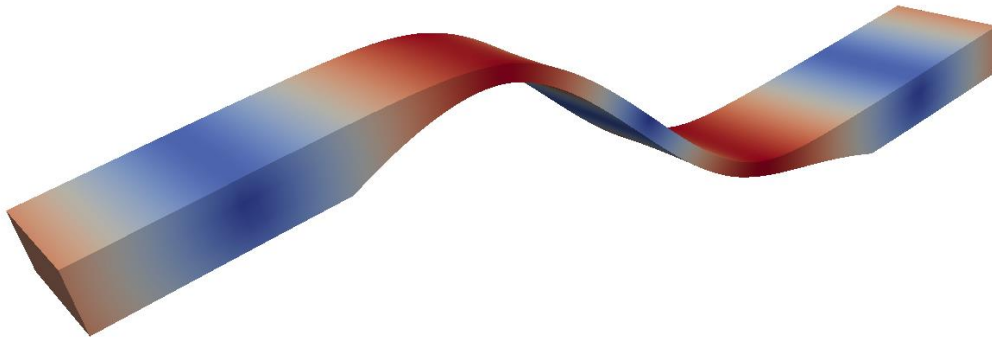


Figure 6: Mode shape #3 from Calculix. The hot-cold colour map indicates overall displacement from blue (minimum) to red (maximum).

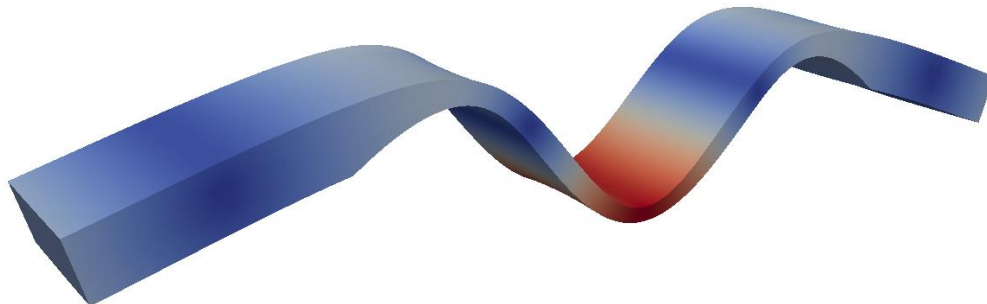


Figure 7: Mode shape #5 from Calculix. The hot-cold colour map indicates overall displacement from blue (minimum) to red (maximum).

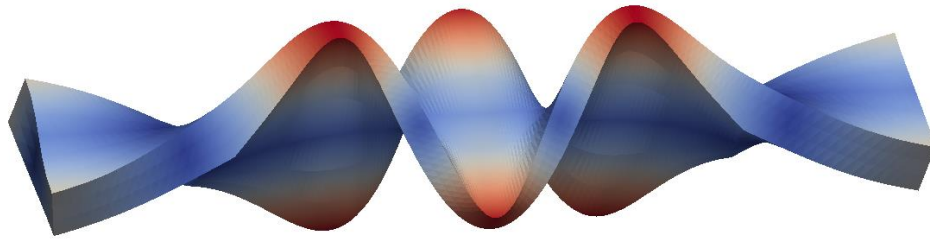


Figure 8: Mode shape #10 from Calculix. The hot-cold colour map indicates overall displacement from blue (minimum) to red (maximum).

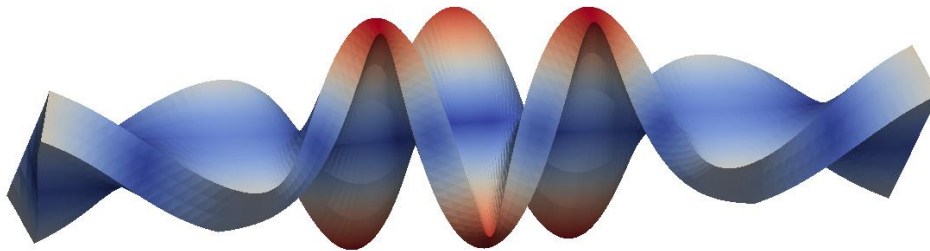


Figure 9: Mode shape #16 from Calculix. The hot-cold colour map indicates overall displacement from blue (minimum) to red (maximum).

Convergence Tests

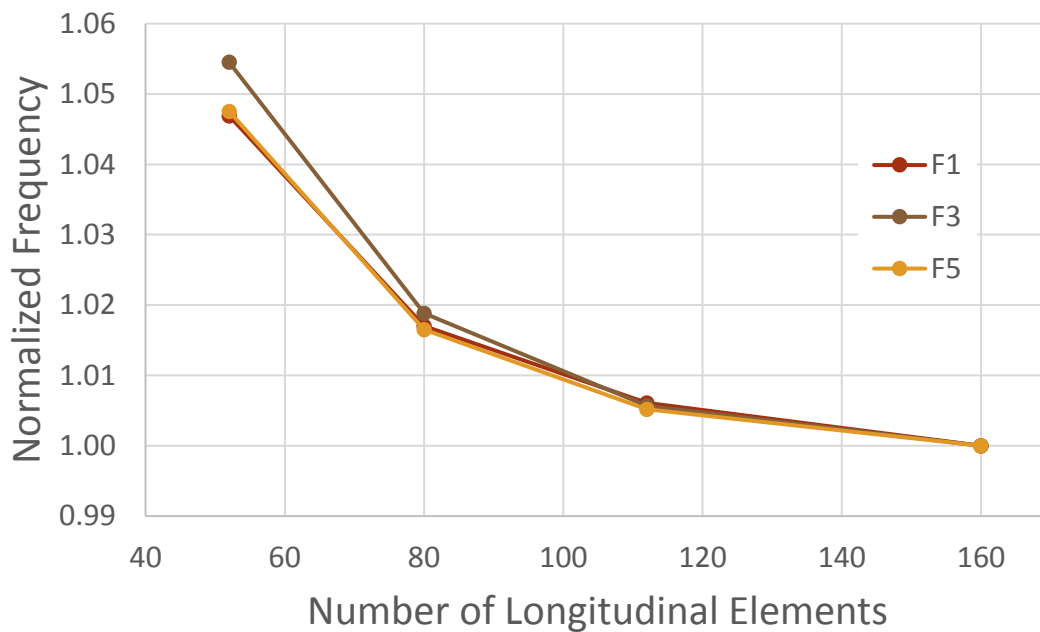


Figure 10: Normalized modal frequencies for Calculix models with various amounts of longitudinal elements. Frequencies are normalized with respect to the model with the most elements. The model by Bork et al. appears at 160 longitudinal elements.

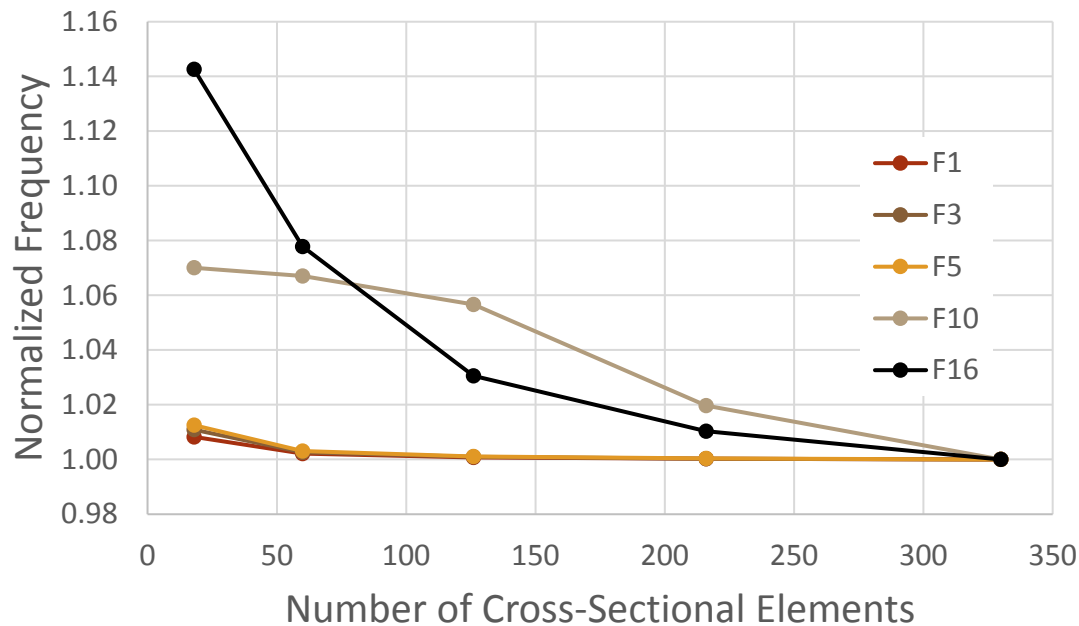


Figure 11: Normalized modal frequencies for Calculix models with various amounts of cross-sectional elements. Frequencies are normalized with respect to the model with the most elements. The model by Bork et al. appears at 21 cross-sectional elements.

Figure 10 and Figure 11 plot normalized modal frequencies from the convergence tests. Each plot shows frequencies for the three tuned modes (F1, F3 and F5), along with some higher order, torsional modes in Figure 11. The number of cross-sectional elements in Figure 11 is the product of the number of elements across the width of the bar and the number of elements through the thickness. In each plot, frequencies are normalized with respect to the model with the most elements. Note the significant difference in vertical axis scale between the two plots.

Discussion

Modal Frequencies and Mode Shapes

As shown in Figure 3, modal frequency results from Calculix follow the same general trend as those from the paper. The fundamental frequency from Calculix is closer to the measured value than the model in the paper. However, the average absolute error from the paper, for modes with both experimental and modelled results, is 2.9%, compared to 4.2% from the Calculix model. The maximum error from Calculix (8.2%) is comparable to that from the paper (7.9%).

Some interesting observations can be made based on the information in Figure 4. First, up to a frequency of about 3.1 kHz, the Calculix model produces frequency results consistently lower than those from the paper. It is possible that the centre portion of the original bar model is not defined with a uniform thickness, and instead gradually tapers to the minimum thickness reported in Table 1. If such is the case, the Calculix model would have less vertical bending stiffness over this important portion of the bar, and we would expect lower modal frequencies as a result.

A second observation from Figure 4 is that the Calculix frequency results for modes 3 and 5 (two of the three tuned modes) are significantly different than those from the paper. While we don't know the exact profile Bork et al. used to model the bar's transition zones, it was likely not the cubic profile used to produce the results shown here. Figure 6 and Figure 7 show the mode shapes for these two modes. It can be observed in these figures, that

for both of these tuned modes, the bar's transition zones are at or near maxima in the displaced shape. For this reason, the transition zone geometry likely has a larger effect on these modes compared to the others.

Finally, we can see from Figure 4 that the general shape of the error curve from Calculix is very similar to that from the paper. In fact, with the exception of the two highest modes (between which the change in error is quite small) the slopes of the error curve from the Calculix model, and the curve from Bork et al. have the same sign everywhere. If these errors were random in nature, to see such a similar pattern throughout the modal frequencies would be quite unexpected. For this reason, it appears the Calculix model has reproduced the essential behaviour of the original model, differing only in a few specific areas due to differences in geometry.

Convergence Tests

In each of Figure 10 and Figure 11, the frequencies shown are normalized with respect to the model with the maximum number of elements in the plot. As such, convergence of the results must be gauged by the relative change in frequency as more elements are added. For this reason, it is important to note the difference in vertical axis scale between Figure 10 and Figure 11.

The model by Bork et al. had 160 elements in the longitudinal dimension, and thus appears as the right-most data points in Figure 10. Looking at the curves in Figure 10, we can see that moving from 112 longitudinal elements to 160 elements (an increase of about 43%) resulted in less than 1% change in frequency for modes 1,3 and 5 (the three tuned modes). As such, 160 longitudinal elements is adequate for modelling these three modal frequencies.

Over the cross-sectional area, the model by Bork et al. had 21 elements (seven across the width by three through the thickness), and so it appears as the left-most data points in Figure 11. Looking at the curves in Figure 11 modes 1, 3 and 5 show about a 1% change in frequency when moving from 21 cross-sectional elements to 60 (an increase of 185%). Beyond 60 cross-sectional elements, using the vertical scale in Figure 11, almost no further change is observable.

Modes 10 and 16 are plotted in Figure 11 to contrast modes 1, 3 and 5. Modes 10 and 16, shown in Figure 8 and Figure 9, respectively, are both higher-order torsional modes and do show significant change in frequency when additional cross-sectional elements are added. As torsional modes they are influenced more heavily by the number of cross-sectional elements than the vertical modes. Also, being higher-order modes, it is expected that they would converge slower than the lower-order modes. Note also that the convergence tests for the cross-sectional elements varied the number of elements across the width and through the thickness simultaneously, and not necessarily by the same factor. This is likely the cause of the atypical shape of the curve for mode 10 in Figure 11.

In light of the above it is evident that modal frequencies for some higher-order modes in Bork et al. [1] would benefit from additional elements in the model. However, the paper did report a ten hour runtime for the model with 2880 elements. For this reason, unless the authors were specifically interested in higher-order torsional mode behaviour, they would not have had much incentive to increase their number of elements (and required runtimes).

Summary

In summary, an interface between the open-source finite element software, Calculix, and the author's software, Pylaster, has been implemented. A model of a marimba bar using 3D finite elements has been defined parametrically in Pylaster, with Calculix serving as the finite element solver via the implemented interface. This bar model matches, as closely as is practical, the model defined by Bork et al. [1].

With limited geometry information provided by Bork et al. a cubic profile was defined to model the bar's "transition zone". This profile was tuned to match the modelled bar mass to the reported mass. Modal analysis was performed to determine the natural frequencies and mode shapes of the modelled bar. The results are comparable to both the experimental modal analysis results and the finite element model results in Bork et al. On average, the error between the Pylaster/Calculix model and the measured results in the paper is slightly larger when compared with the model in the paper. This difference in results is most likely attributable to the assumptions and approximations required to define the model, in light of the limited information provided by the paper.

Convergence tests were performed on the model. These tests varied either the number of elements in the longitudinal direction, or the number of elements over the cross-section of the bar. The results show that, using the number of elements specified in the paper, the frequencies of modes 1, 3 and 5 (those modes typically tuned in a marimba bar) appear to have converged to within a reasonable tolerance. The convergence tests also show that some higher-order torsional modes may not yet have converged using that same mesh. However, in the absence of a specific interest in higher-order torsional modes, the additional runtime required for this model (circa 1999) would not have warranted additional elements.

Overall the model has successfully demonstrated Calculix's capacity for modal analysis, and confirmed the quality of the original work by Bork et al.

References

- [1] I. Bork, A. Chaigne, L.-C. Trebuchet, M. Kosfelder and D. Pillot, "Comparison between Modal Analysis and Finite Element Modelling of a Marimba Bar," *Acta Acustica united with Acustica*, vol. 85, no. 2, pp. 258-266, 1999.